Trace metal analysis ofelement on material surfaceusing pulse CO2 laser-inducedbreakdown spectroscopyapplying vaporization technique

by Ali Khumaeni

Research article

Trace metal analysis of element on material surface using pulse CO_2 laser-induced breakdown spectroscopy applying vaporization technique

Ali Khumaeni [a,*], Wahyu Setia Budi [a], Kazuyoshi Kurihara [b], Hendrik Kurniawan [c], Kiichiro Kagawa [d]

[a] Department of Physics, Faculty of Science and Mathematics, Diponegoro University, Semarang 50275, Indonesia
[b] Department of Physics, Faculty of Education, University of Fukui, Bunkyo 3-9-1, Fukui 910-8507, Japan
[c] Maju Makmur Mandiri Research Center, Kembangan, Jakarta Barat, Indonesia
[d] Fukui Science Education Academy, Takagi Chuo 2 chome, Fukui 910-0804, Japan

ARTICLE INFO

ABSTRACT

Trace elemental analysis on a surface of material has been recently imperative to be carried out especially in material industries. In this study, sophisticated setup of laser-induced breakdown spectroscopy has been arranged and demonstrated by employing vaporization technique for the trace elemental analysis on a surface of material without ablating the material itself. Experimentally, a pulse transversely excited atmospheric CO_2 laser was directed and defocused at +5 mm on a Si surface at inclining degree of approximately 25° to vaporize the trace metal element from the Si surface to the Pt mesh combined with Cu plate. The vaporized trace metal element then attached and deposited on the mesh surface. The trace metal attached-Pt mesh was then bombarded by focused laser beam to induce a luminous plasma and finally the trace element was identified. Results certified that sensitive trace elemental analysis of Cr deposited on the Si surface has been successfully carried out without any ablation of Si surface. Good linear calibration curve of Cr with an intercept zero was produced, which results in limit of detection of Cr of approximately 100 ppb.

1. Introduction

Trace elemental analysis is urgently necessary in various fields including environmental field and material industries. In environmental science, trace elemental analysis of soil has attracted interest many researchers as reported in elsewhere [1, 2, 3, 4, 5]. The analysis of trace element is also required in material industries because the trace contaminants in materials influence the electrical conduction of the material itself [6, 7, 8, 9, 10].

One of standard spectroscopic techniques used for the elemental analysis on the surface of material target is X-ray PhotoelectronSpectroscopy (XPS). This technique is based on the photoelectric effect, which is able to identify the elements present within a material. XPS has been applied to identify elements in inorganic compound, metal alloys, and semiconductors [11, 12, 13, 14]. The other technique is X-ray Diffraction Spectroscopy (XRD) [15, 16]. It offers rapid analysis, but the detection sensitivity is quiet low.

The interesting method recently applied to the trace elemental analysis in materials is laser-induced breakdown spectroscopy (LIBS). In LIBS, a pulse Nd:YAG laser is commonly applied to generate a plasma on a sample surface [17, 18, 19]. Some researchers used pulse CO_2 laser to generate plasma, which has long lifetime and large volume [20, 21, 22]. The LIBS method based on Nd:YAG and CO_2 lasers has been employed in many kinds of materials [23, 24, 25, 26]. Recently, the LIBS system has been employed for analysis of trace elements in liquids and semiconductors [27, 28, 29]. Compared to other standard conventional method, LIBS is most rapid analytical technique and does not need complicated sample preparation. However, it suffers from good sensitivity because of the effect of sample matrix.

To improve the detection sensitivity, some researchers employed double pulse laser induced breakdown spectroscopy (DP-LIBS), in which one laser is applied to generate an initial plasma and the remaining one is functioned to reheat the plasma induced by first laser [30, 31, 32, 33]. Many applications of DP-LIBS have been conducted including analysis of various materials including metals and semiconductors [34, 35]. However, based on our experience, DP-LIBS applications for elemental analysis is tedious in experimental preparation and quiet expensive due to requirement of additional laser system [36].

In the other direction, unique circumstance happens when the radiation source of pulse Nd:YAG laser is replaced by a pulse transversely excited atmospheric (TEA) CO_2 laser. Namely, long-lifetime and large-volume plasma is generated because of longer wavelength and longer pulse duration, resulting in higher plasma absoprtion [37, 38]. We have used the TEA CO_2 laser-induced breakdown spectroscopy (TEA CO_2 LIBS) for many applications including analyses of soils, powders, and softwood as presented here [39, 40, 41, 42].

Expanding the TEA CO_2 LIBS technique, we further employed to trace elemental analysis of silicon [43]. However, the technique is still lack of sensitivity because the silicon material itself was ablated. Furthermore, the ablation of the Si material makes the material itself damaged, which is avoided in analysis of trace element on semiconductor material. To overcome this issue, in this present paper, we proposed new technique of vaporization utilizing a TEA CO_2 LIBS for trace elemental analysis of Si material without damaging the material itself, which is necessary in material industries. The technique consists of two steps, namely vaporization and data acquisition. For vaporization, the trace metal impurity attached on the surface of material was vaporized and deposited onto the Pt metal mesh and metal subtarget by defocusing a pulse CO_2 laser beam on the material, which contains trace metal. In the second step, the deposited trace metal elements was then irradiated by a CO_2 laser beam to induce a plasma, obtaining emission spectrum of trace metal element. Using new present technique, trace metal analysis on a surface of material can successfully be carried out without damaging the material itself, which is necessary in material industries. The detection sensitivity of impurity element is also high in the order of sub part per million (ppm) level.

2. Experimental procedure

The material target used was silicon wafers with a thickness of 0.5 mm and a diameter of 51 mm. The silicon wafers contain Cr at a various concentrations as a trace element on its surface. For example, to produce Cr film at a concentration of 1.25 mg/kg, the same procedure with the previous experiment [43] was conducted.

The basic setup is illustrated in Figure 1(b) and (c). The setup consisted of two steps, namely new vaporization technique (Figure 1(b)) and data acquisition (Figure 1(c)). In vaporization technique, two sheets of platinum metal mesh (wire diameter of 0.12 mm and lattice constant of 0.50 mm) were tightly attached on a copper plate ($0.1 \times 2 \times 2$ mm^3). The meshes were then placed at 10 mm in front of the Si wafer, which contains impurity on its surface, as displayed in Figure 1(b). The Si wafer was placed on a sample holder, which can be rotated during laser bombardment. The TEA CO_2 laser (10.64 um, 200 ns, 750 mJ) was directly bombarded and defocused at $+5$ mm by using a ZnSe lens (200 mm in focal length) onto the Si wafer surface. The irradiance of the laser beam on the Si wafer surface was 0.09 GW/cm^2. It should be mentioned that no plasma emission was produced during laser bombardment and only the impurity on the Si surface is vaporized onto the surface of the Pt metal meshes. During laser bombardment, the wafer was continuously rotated with a rotation speed of 2 rotations per minute (rpm). This procedure was made to convince that the laser beam always attaches new position on the wafer surface and therefore, the impurity optimally vaporizes and moves to deposit and accumulate on the mesh surface. For data acquisition, the meshes on which the impurity is deposited, was placed into the alloy chamber (diameter of 12 cm). During acquisition, the impurity-deposited mesh was rotated with a rotation rate of 2 rpm. He gas (99.999%) was flown into the chamber with a flow rate of 10 L/min. The pressure inside the chamber was kept constant at 1 atmospheric pressure. The pulse TEA CO_2 laser with a laser energy of 1500 mJ was focused on the mesh surface by using ZnTe lens with a focal length of 200 nm. The laser beam irradiance on the mesh surface was 0.75 GW/cm^2. A luminous plasma was then generated just above the mesh surface.

The emission spectrum was obtained by multichannel analyzer (ATAGO Macs-320, 1024-channel detector, OMA) from the plasma
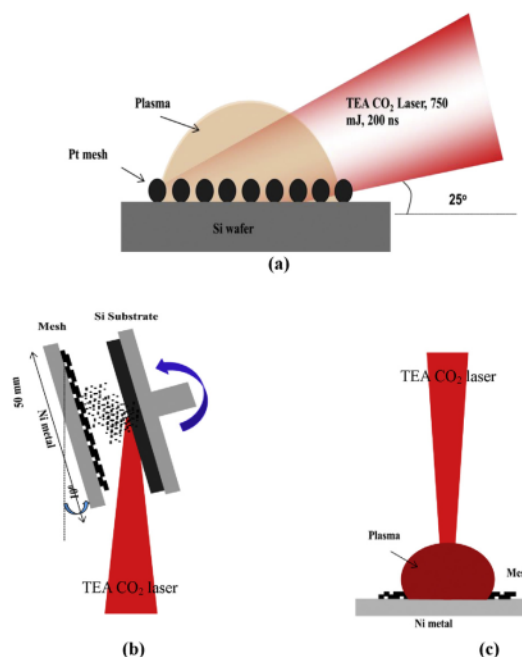

Figure 1. Illustration of Experimental setup used in this study (a) by inclining technique, (b) and (c) by vaporization technique.

emission, which is sent into the optical fiber that connects to the OMA system. The spectrum was gained by 10 shots of laser bombardment. In experiment, delay time and gate width of OMA were 10 μs and 200 μs, respectively. For plasma emission studies, a delay time was selected at 10 μs. This is because in laser plasma induced by a pulse TEA CO_2 laser (10.64 um, 200 ns, 1500 mJ), the best spectral quality, namely narrow full width at half-maximum (FWHM) and optimum signal to noise (S/N) ratio with low background continuum emission is obtained at around 10 μs [38]. Below 10 μs, the FWHM is still quiet wide and background continuum is still high. The background continuum emission, which is produced by Bremsstrahlung effect (free-free) and recombination (free-bound transition), has long lifetime up to around 10 μs compared to that of plasma emission produced by Nd:YAG laser, which has background continuum emission up to around 1 μs. In laser-induced breakdown spectroscopy (LIBS), FWHM of emission line, S/N ratio, and background emission determine the spectral quality and thus influence the sensitivity.

3. Results and discussion

Unique circumstance happens when the TEA CO_2 laser beam is focused on metal sample. Namely, a large volume and long lifetime plasma was induced without any ablation of the metal surface. The plasma is most often contributed from the surrounding gas, not from the material target, and therefore, we called "gas plasma" as reported in our previous works [38]. By this present method, identification and analysis of impurity in various sample target has been successfully made.

To extend the significance of the method, in this present study, identification of trace metal element on a material Si surface was made. As mentioned in introduction, analysis of trace element on a material surface without any damaging the material itself is very necessary especially in semiconductor industry. At initial study, to avoid the ablation of Si itself by a laser bombardment, a platinum metal mesh (wire diameter of 0.12 mm and lattice constant of 0.50 mm) was employed by tight attaching the mesh on the Si surface and by directing a laser beam

onto the Si surface at the angle 25°from the Si surface so that the laser beam does not directly impinge on the Si surface. The pulse TEA CO_2 laser beam (10.64 um, 200 ns, 750 mJ) was further focused onto the surface of Pt mesh at inclining degree of 25° to induce a luminous plume (Figure 1(a)). Mixed nitrogen and helium gases with a flow rate of 2.5 L per minute were flowed during data acquisition process. Figure 2 shows an emission spectrum obtained from the silicon surface containing trace metal element of 1.25 ppm Cr at the wavelength region of 410 nm–440 nm. Typical neutral Cr lines at the wavelength of 425.4 nm, 427.4 nm, and 428.9 nm are clearly identified together with neutral Ca line at 422.6 nm. Furthermore, a high-intensity broaden emission line at 434.0 nm identified as $H_\gamma$line. This result certified that even though the laser beam was sent at the angle of 25° from the Si surface, the Cr impurity deposited on the Si surface still can be vaporized and excited in the plasma region indicated by detection of Cr lines as in the spectrum.

Further experiment was made to confirm whether any ablation happens from the Si surface. As mentioned above, the important goal of the study is to identify and analysis of trace metal element on Si surface without any damage on the Si material itself. Figure 3 displays an emission spectrum taken from the same condition with Figure 2 at the wavelength region ranging from 270 nm to 310 nm. Neutral atomic Si line at 288.2 nm faintly appears together with high-intensity neutral He line. The weak line of Si 288.2 nm is most often because of experimental setup, which we proposed in this study, namely, by inclining the laser beam at inclining degree of 25°coming onto the Si surface, which is attached by a metal mesh just on the Si surface. By using this technique, the ablation of the material sample can effectively be reduced due to shadow effect by a metal mesh as reported in our previous paper [43]. The existence of Si line verified that the Si material is still ablated by direct laser bombardment in the present method, thus resulting in material damaged. It should be mentioned that when the inclining degree of the metal mesh to the surface of the Si was reduced from 25° to 10°, the emission line of Si at 288.2 nm significantly decreased and almost disappeared, which stated that the ablation of the Si material also decreased. However, the reduction of the Si ablation also reduces significantly the emission lines of Cr impurity at the wavelength of 325.4 nm, 327.4 nm, and 328.9 nm. Therefore, the present technique is not sensitive to be employed for the detection of impurity deposited on the material surface, especially Si surface. Furthermore, this technique cannot effectively be employed to perform analysis of trace element on material without damaging the material itself, which is required in semiconductor industry.

A new devised technique was then proposed to overcome the problem of the material ablation and reduction of the impurity emission lines. The technique consists of two steps as shown in Figure 1(b) and (c), namely vaporization and data acquisition. In the first step (Figure 1(b)), a defocused laser beam at +5 mm was sent onto the Si surface to vaporize the trace element from the Si surface to move on the Pt metal mesh. We confirmed that completely no plasma was generated on the surface of Si
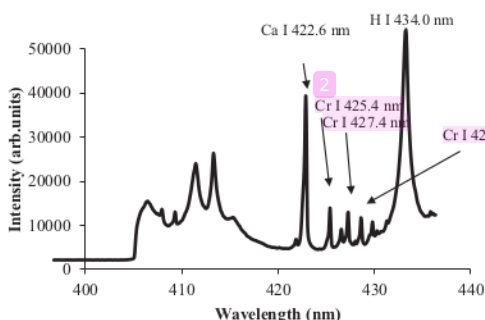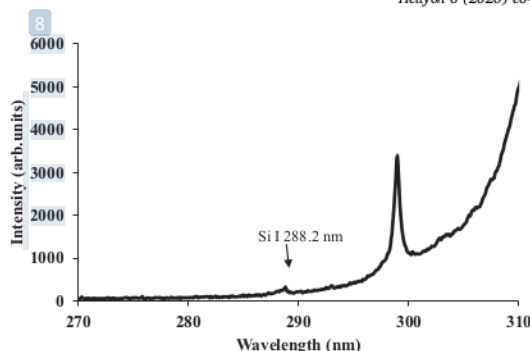

Figure 3. Emission spectrum of Si taken from the Si wafer containing Cr at 1.25 ppm using inclining technique.

and no Si line at 288.2 nm was detected during defocusing of the laser beam. Also, no ablation mark on the Si surface was observed by the microscope. In the data acquisition step (Figure 1(c)), the trace-element deposited-metal mesh and Cu plate was bombarded by the focused laser beam to generate a plasma and to identify the trace element emission. It should be stated that the mesh and Cu plate was not ablated by the laser beam because the power density on their surface is not high enough to ablate the metal as shown in our paper [40]. The plasma emission induced was totally contributed from the surrounding gas and the trace element deposited on the surface. We clearly observed the luminous plasma and detected the emission lines of trace elementof Cr and H_γ emission as shown in Figure 4. The H_γ emission line might be contributed from the sugar solution used during sample preparation process as described in experimental procedure. The sample used was Si wafer containing Cr impurity on the Si surface at 4 ppm. Three typical emission lines of neutral Cr at 425.4 nm, 427.4 nm, and 428.9 nm appears with high intensity and quite low background emission even at low concentration of 4 ppm level. These lines are contributed from the trace element of Cr deposited on the Si surface. In addition, high-intensity and broaden emission line of H_γ at 434.0 nm and neutral Ca line at 422.6 nm contributed from the sugar solution and tap water clearly occurs.

Prior to semi-quantitative analysis of Cr trace element deposited on Si surface, the characteristics of plasma emission such as temperature and electron density were calculated. By considering that the population densities of the higher energy levels of two emission lines are in LTE condition, the calculation of electron temperature (Te) can be derived by the intensity ratio method [44]. In this study, the Te was obtained from the hydrogen lines of Balmer region using Eq. (1) as follows,

$$T_e = \frac{\Delta E}{\ln \frac{[A_1 g_1 \lambda_2 I_2]}{[A_2 g_2 \lambda_1 I_1]} K} \quad (1)$$

Figure 2. Emission spectrum of Cr deposited on the surface of silicon wafer containing 1.25 ppm Cr using inclining technique.
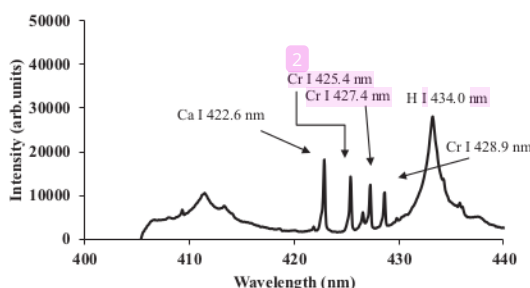
Figure 4. Emission spectrum of Cr obtained from the Si wafer surface containing Cr at 4 ppm using vaporization technique.
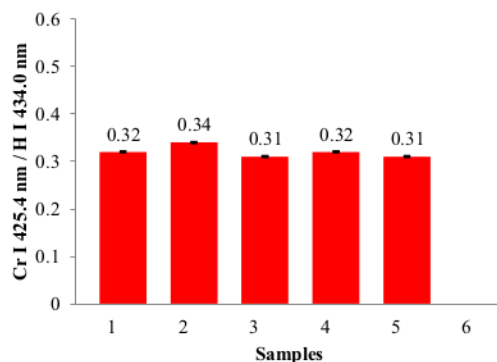
Figure 5. Reproducibility of H_γ emission obtained from the gas plasma produced on the surface of Si wafer containing 4 ppm Cr.

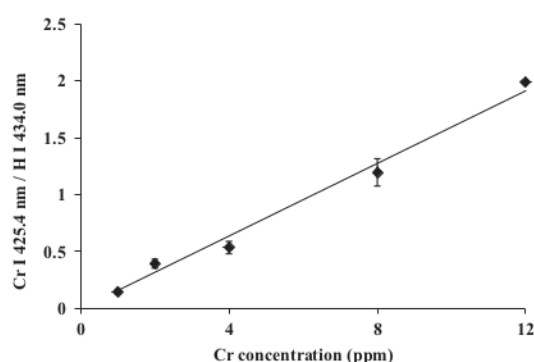**Figure 6.** Calibration curve of Cr deposited on the Si surface at various concentrations by using the vaporization technique.

where ΔE, λ, I, A, g, and K are the energy difference between two levels, wavelength, intensity, transition probability, statistical weighting factor, and Boltzmann constant and respectively. Two hydrogen emission lines of Balmer-γ and Balmer-δ were used and all parameter values were obtained from the NIST database [45]. Based on Eq. (1), the electron temperature was approximately 5000 K. The electron density was determined using the stark broadening theory, The electron density (Ne) was obtained from the linewidth of hydrogen lines using Eq. (2) as follows [46],

$$N_e = 8.02x10^{12}\left[\frac{\Delta\lambda_{1/2}}{\alpha_{1/2}}\right]^{3/2} \tag{2}$$

where reduced wavelength $\alpha_{1/2}$ is a function of the electron density and temperature and $\Delta\lambda_{1/2}$ is the linewidth of FWHM in angstroms. Reduced wavelength $\alpha_{1/2}$ for the Balmer series is obtained from the report here [47]. Using Eq. (2), the Ne was to be in the order of 10^{17} cm^{-3}.

Finally, a semi-quantitative analysis of Cr has been carried out by using the Si sample containing different concentrations of Cr on Si wafer surface. Prior to analysis, reproducibility of the gas emission was examined using the H_γ at 434.0 nm As shown in Figure 5, with the number of laser shots at different places on the surface of metal mesh and Cu plate, on which the Cr impurity was deposited, good reproducibility of the H_γ emission is obtained. This graph certified that the plasma produced using this present technique is quite stable and therefore it is feasible for the semi-quantitative analysis of Cr trace element in the Si surface. The good reproducibility of the H_γ at 434.0 nm was then used as a standard line for making the calibration.

Figure 6 displays the calibration curve for Cr in the Si surface. In this graph, Cr line at 425.4 nm was selected because this line has highest intensity compared to other Cr line. Good linearity with zero intercept was obtained between emission ratio of Cr to H_γ and Cr concentration deposited on the Si surface. Using the same equation for calculating the limit of detection (LoD) as reported here [48], the LoD of Cr was around 100 ppb; The LoD was derived from the emission intensity of analyte which yielded 3 times the noise level because this was clearly identified as an analyte signal that could be distinguished from the noise. This result stated that the present vaporization technique is applicable to high-sensitivity analysis of trace element on material surface.

4. Conclusion

A vaporization technique consisting of two step process utilizing a pulse TEA CO_2 laser has been established and demonstrated for the identification impurity element of Cr deposited on material surface of Si. Good stability of the plasma emission was investigated. Using the present technique, a semi-quantitative analysis of Cr on a Si wafer surface was successfully made. A good linearity calibration curve of Cr using H_γ emission line as a standardization with an intercept zero was demonstrated. The limit detection of Cr was approximately 100 ppb. The present technique is potentially applied to analysis of impurity on material surface in material science and industry.

References

[1] L. Ciadamidaro, M. Puschenreiter, J. Santner, W.W. Wenzel, P. Madejon, E. Madejon, Assesment of trace element phytoavailability in compost amended soils using different methodolies, J. Soils Sediments 17 (2017) 1251–1261.

[2] P. Abad-Valle, E. Iglesias-Jimenez, E. Alvarez-Ayuso, A comparative study on the influence of different organic amendments on trace element mobility and microbial functionality of a polluted mine soil, J. Environ. Manag. 188 (2017) 287–296.

[3] J.L. Cui, C.L. Luo, C.W. Tang, T.S. Chan, X.D. Li, Speciation and leaching of trace metal contaminants from e-waste contaminated soils, J. Hazard Mater. 329 (2017) 150–158.

[4] V.M. Ngole-Jeme, G.I.E. Ekosse, S.P. Songca, An analysis of human exposure to trace elements from deliberated soil ingestion and associated health risks, J. Expo. Sci. Environ. Epidemiol. 28 (2018) 55–63.

[5] Z. Ding, Y. Li, Q. Sun, H. Zhang, Trace elements in soils and selected agricultural plants in the Tongling Mining area of China, Int. J. Environ. Res. Publ. Health 15 (2018) 202.

[6] J. Wang, M.K. Balazs, P. Pianetta, K. Baur, S. Brennan, Analytical Techniques for Trace Elemental Analyses on Wafer Surfaces for Monitoring and Controlling Contamination. Semiconductor Pure Water and Chemicals Conference 19th, 2000, p. 400.

[7] S. Liu, B. Liu, Characterization of cleanroom dry wipers for trace metal contaminations, Ecs.J. Solid State Sci. Technol. 3 (2014) N3087–N3094.

[8] C. Neumann, P. Eichinger, Ultra-trace analysis of metallic contaminants on silicon wafer surface by vapour phase decomposition/total reflection X-ray fluorescence (VPD/TXRF), Spectrochim. Acta, Part B 46 (1991) 1369–1377.

[9] S. Pahlke, L. Fabry, L. Kotz, C. Mantler, T. Ehmann, Determination of ultra trace contaminants on silicon wafer surfaces using total-reflection X-ray fluorescence TXRF 'state of the art', Spectrochim. Acta Part B 56 (2001) 2261–2274.

[10] P. Rostam-Khani, M.J.P. Hopstaken, P. Vullings, G. Noij, O. O'Halloran, W. Claassen, Quantification issues of trace metal contaminants on silicon wafers by means of TOF-SIMS, ICP-MS, and TXRF, Appl. Surf. Sci. 231–232 (2004) 720–724.

[11] V. Gupta, H. Ganegoda, M.H. Engelhard, J. Terry, M.R. Linford, Assigning oxidation states to organic compounds via predictions from x-ray photoelectron spectroscopy: a discussion of approaches and recommended improvements, J. Chem. Educ. 91 (2013) 232–238.

[12] J. Halim, K.M. Cook, M. Naguib, P. Eklund, Y. Gogotsi, J. Rosen, M.W. Barsoum, X-ray photoelectron spectroscopy of selec multi-layered transition metal carbides (MXenes), Appl. Surf. Sci. 362 (2016) 406–417.

[13] B.P. Payne, M.C. Biesinger, N.S. McIntyre, X-ray photoelectron spectroscopy studies of reactions on chromium metal and chromium oxide surface, J. Electron. Spectrosc. 184 (2011) 29–37.

[14] M. Perego, G. Seguini, Charging phenomena in dielectric/semiconductor heterostructures during x-ray photoelectron spectroscopy measurements, J. Appl. Phys. 110 (2011), 053711.

[15] U. Kalsoom, S. Bashir, N. Ali, SEM, AFM, EDX, and XRD analysis of laser ablated Ti in nonreactive and reactive ambient environments, Surf. Coat. Tech. 235 (2013) 297–302.

[16] Z. Demircioğlu, Ç.A. Kaştaş, O. Büyükgüngör, XRD, FT–IR and UV characterization, hirshfeld surface analysis and local-global chemical descriptor studies of (E)-2-((3-fluorophenylimino)methyl)-3-methoxyphenol (1) and (E)-2-((2-fluorophenylimino) methyl)-3-methoxyphenol (2), J. Mol. Struct. 1166 (2018) 131–146.

[17] Q. Wang, X. Cui, G. Teng, Y. Zao, K. Wei, Evaluation and improvement of model robustness for plastic samples classification by laser-induced breakdown spectroscopy, Optic Laser. Technol. 125 (2020) 106035 1–9.

[18] Z.X. Lin, L.M. Liu, L.W. Liu, Validation of the solidifying soil process using laser-induced breakdown spectroscopy, Optic Laser. Technol. 83 (2016) 13–15.

[19] J.P. Singh, S.N. Thakur, Laser-induced Breakdown Spectroscopy, Elsevier, Oxford, 2007.

[20] E. Bellou, N. Gyftokostas, D. Stefas, O. Gazeli, S. Couris, Laser-induced breakdown spectroscopy assisted by machine learning for olive oils classification: the effect of the experimental parameters, Spectrochim. Acta Part B 163 (2020) 105746.

[21] C.G. Parigger, J.O. Hornkohl, L. Nemes, Time-resolved spectroscopy diagnostic of laser-induced optical breakdown, Int. J. Spectrosc. 2010 (2010) 593820.

[22] S. Zivkovic, J. Savovic, M. Trtica, J. Mutic, M. Momcilovic, Elemental analysis of aluminum alloys by laser induced breakdown spectroscopy based on TEA CO2 laser, J. Alloys Compd. 700 (2017) 175–184.

[23] M. Weidman, M. Baudelet, S. Palanco, M. Sigman, P.J. Dagdigian, M. Richardson, Nd:YAG-CO2 double-pulse laser induced breakdown spectroscopy of organic films, Opt. Express 18 (2010) 259–266.

[24] N. Farid, C. Li, H. Wang, H. Ding, Laser-induced breakdown spectroscopic characterization of tungsten plasma using the first, second, and third harmonics of an Nd:YAG laser, J. Nucl. Mater. 433 (2013) 80–85.

[25] M. Momcilovic, M. Trtica, J. Ciganovic, J. Savovic, J. Stasic, M. Kuzmanovic, Analysis of copper surface features obtained using TEA CO2 laser at reduced pressure, Appl. Surf. Sci. 270 (2013) 486–494.

[26] S. Polić, S. Ristić, J. Stašić, M. Trtica, B. Radojković, Studies of the Iranian medieval ceramics surface modified by pulse TEA CO2 and Nd:YAG lasers, Ceram. Int. 41 (2015) 85–100.

[27] C. Du, X. Liu, W. Miao, X. Cheng, Investigation on laser-induced breakdown spectroscopy of MgCl2 solution, Optik 187 (2019) 98–102.

[28] A.H. Galmed, A.K. Kassem, H.V. Bergmann, M.A. Harith, A study of using femtosecond LIBS in analyzing metallic thin film-semiconductor interface, Appl. Phys. B 102 (2011) 197–204.

[29] S.A. Davari, P.A. Taylor, R.W. Standley, D. Mukherjee, Detection of interstitial oxygen contents in Czochralski grown silicon crystals using internal calibration in laser-induced breakdown spectroscopy, Talanta 193 (2019) 192–198.

[30] P.K. Diwakar, S.S. Harilal, J.R. Freeman, A. Hassanein, Role of laser pre-pulse wavelength and inter-pulse delay on signal enhancement in collinear double-pulse laser-induced breakdown spectroscopy, Spectrochim. Acta B 87 (2013) 65–73.

[31] K. Rifai, S. Laville, F. Vidal, M. SAbsabi, M. Chaker, Quantitative analysis of metallic traces in water-based liquids by UV-IR double-pulse laser-induced breakdown spectroscopy, J. Anal. At. Spectrom. 27 (2012) 276–283.

[32] I.Y. Elnasharty, F.R. Doucet, J.-F. Gravel, P. Bouchard, M. Sabsabi, Double-pulse LIBS combining short and long nanosecond pulses in the microjoule range, J. Anal. At. Spectrom. 29 (2014) 1660–1666.

[33] L. Sun, H. Yu, Z. Cong, Y. Xin, Y. Li, L. Qi, In situ analysis of steel melt by double-pulse laser-induced breakdown spectroscopy with a Cassegrain telescope, Spectrochim. Acta B 112 (2015) 40–48.

[34] A.A.I. Khalil, Chemmical etching method assisted double-pulse LIBS for the analysis of silicon crystal, Appl. Phys. A 119 (2015) 1087–1099.

[35] J. Guo, T. Wang, J. Shao, T. Sun, R. Wang, A. Chen, Z. Hu, M. Jin, D. Ding, Emission enhancement ratio of the metal irradiated by femtosecond double-pulse laser, Optic Commun. 285 (2012) 1895–1899.

[36] E. Tognoni, G. Cristoforetti, Basic mechanism of signal enhancement in ns double-pulse laser-induced breakdown spectroscopy in a gas environment, J. Anal. At. Spectrom. 29 (2014) 1318–1338.

[37] Z.S. Lie, A. Khumaeni, K. Kurihara, K.H. Kurniawan, Y.I. Lee, K. Fukumoto, K. Kagawa, H. Niki, Excitation mechanism of H, He, C, and F atoms in metal-assisted atmospheric helium gas plasma induced by transversely excited atmospheric-pressure CO2 laser bombardment, Jpn. J. Appl. Phys. 50 (2011) 122701.

[38] A. Khumaeni, Z.S. Lie, H. Niki, K.H. Kurniawan, E. Tjoeng, Y.I. Lee, K. Kurihara, Y. Deguchi, K. Kagawa, Direct analysis of powder samples using transversely excited atmospheric CO2 laser-induced gas plasma at 1 atm, Anal. Bioanal. Chem. 400 (2011) 3279–3287.

[39] A. Khumaeni, Z.S. Lie, Y.I. Lee, K. Kurihara, K. Kagawa, H. Niki, Rapid analyses of tiny amounts of powder samples using transversely excited atmospheric CO2 laser-induced helium gas plasma with the aid of high-vacuum silicon grease as a binder on a metal subtarget, Appl. Spectrosc. 65 (2011) 236–241.

[40] A. Khumaeni, M. Ramli, N. Idris, Y.I. Lee, K.H. Kurniawan, T.J. Lie, Y. Deguchi, H. Niki, K. Kagawa, Rapid quantitative analyses of elements on herb medicine and food powder using TEA CO2 laser-induced plasma, in: AIP Conference Proceedings, Vol. 1104, 2009, pp. 155–160.

[41] A. Khumaeni, H. Niki, Y. Deguchi, K. Kurihara, K. Kagawa, Y.I. Lee, Analysis of organic powder samples by using metal-assisted subtarget effect in a Transversely-Excited Atmospheric (TEA) CO2 laser-induced He gas plasma at 1 atm, J. Kor. Phys. Soc. 55 (2009) 2441–2446.

[42] A. Khumaeni, Z.S. Lie, H. Niki, Y.I. Lee, K. Kurihara, M. Wakasugi, T. Takahashi, K. Kagawa, Comparative study of Nd:YAG laser-induced breakdown spectroscopy and transversely excited atmospheric CO2 laser-induced gas plasma spectroscopy on chromate copper arsenate preservative-treated wood, Appl. Optic. 51 (2012) B121–B129.

[43] A. Khumaeni, W.S. Budi, Z.S. Lie, K.H. Kurniawan, K. Kurihara, K. Kagawa, Pulse CO2 laser-induced gas plasma spectroscopy based on single beam splitting for trace metal analysis on a material surface, J. Mod. Optic. 65 (2018) 2195–2199.

[44] M.W. Ahmeda, M.S. Rahmana, S. Choia, U. Shaislamovb, J.-K. Yanga, R. Suresha, H.-J. Lee, Measurement of electron temperature and nnumber density and their effects on reactive species formation in a DC underwater capilarry discharge, Appl. Sci. Coberg. Technol. 26 (2017) 118–128.

[45] https://www.nist.gov/pml/atomic-spectra-database.

[46] J. Ashkenazy, R. Kipper, M. Caner, Spectrocopic measurements of electron density of capillary plasma based on Stark broadening of hydrogen lines, Phys. Rev. A 43 (1991) 5568–5574.

[47] P. Kepple, H.R. Griem, Improved Stark profile calculations for the hydrogen lines Hα, Hβ, Hγ, and Hδ, Phys. Rev. 173 (1968) 317–325.

[48] J.D. Ingle Jr., S.R. Crouch, Spectrochemical Analysis, Prentice Hall, New Jersey, 1988.

C2 - Trace metal analysis of element on material surface using pulse CO2 laser-induced breakdown spectroscopy applying vaporization technique

| 7 | infoscience.epfl.ch
Internet Source | <1 % |
| 8 | research-repository.st-andrews.ac.uk
Internet Source | <1 % |

| Exclude quotes | Off | Exclude matches | Off |
| Exclude bibliography | On | | |